HHS Public Access

Author manuscript

Chem Commun (Camb). Author manuscript; available in PMC 2016 April 08.

Published in final edited form as:

Chem Commun (Camb). 2015 February 11; 51(12): 2235–2238. doi:10.1039/c4cc06165a.

The coaction of tonic and phasic dopamine dynamics

Christopher W. Atcherley[1,*], **Kevin M. Wood**[2,*], **Kate L. Parent**[1], **Parastoo Hashemi**[2,†], and **Michael L. Heien**[1,†]

[1]Department of Chemistry and Biochemistry, University of Arizona, 1306 East University Boulevard, Tucson, AZ 85721, United States of America

[2]Department of Chemistry, Wayne State University, 5101 Cass Avenue, Detroit, MI 48202, United States of America

Abstract

Tonic neurochemical dopamine activity underlies many brain functions; however a consensus on this important concentration has not yet been reached. In this work, we introduce *in vivo* fast-scan controlled-adsorption voltammetry to report tonic dopamine concentrations (90 ± 9 nM) and the dopamine diffusion coefficient (1.05 ± 0.09 ×10^{-6} cm^2/s) in the mouse brain.

Dopamine signalling involves slow, tonic brain activity that regulates the steady-state extracellular concentration of dopamine, while rapid or phasic neuronal firing accompanies salient stimuli.[1,2] Importantly, dopamine receptor occupancy, transporter function, and synaptic plasticity are critically dependent on the tonic concentration of dopamine in the extracellular space.[1,3,4] Therefore, making tonic *in vivo* measurements is essential for establishing dopamine's physiological mechanisms and the pathophysiological abnormalities underlying disorders and diseases such as Parkinson's, schizophrenia, and addiction.[5,6] To measure tonic concentrations, researchers have relied on either microdialysis[7–9] or pairing pharmacology to fast-scan cyclic voltammetry (FSCV) at carbon-fiber microelectrodes.[10–13] Using these methods, tonic levels of dopamine have been reported in the range of 1 nM to 2.5 μM.[2,14–16] Such a wide range of values can be attributed to physical limitations in microdialysis,[9,17] tissue damage,[18,19] or experimental assumptions inherent in pharmacological hypotheses. A direct *in situ* technique would greatly aid researchers to more accurately decipher dopamine neurochemistry.

Carbon-fiber microelectrodes are an ideal sensor for *in vivo* measurements because of their biocompatibility, minimally intrusive dimensions (Ø = 7 μm, length = 50 μm), and rapid response time.[11,12,20] When paired with FSCV, these sensors are restricted from directly measuring tonic dopamine levels because background-subtraction is required to remove a large background current, allowing only rapid changes to be quantified.[21] In this work, we overcome this limitation and validate a novel method, fast-scan controlled-adsorption voltammetry (FSCAV) at carbon-fiber microelectrodes to, for the first time, directly measure tonic dopamine concentrations *in situ* with high selectivity, sensitivity, and temporal

†To whom correspondence should be addressed: mheien@arizona.edu, phashemi@chem.wayne.edu.
*Contributed equally to this work

resolution. Further, FSCAV is used to map dopamine diffusion through the tissue surrounding the electrode and to determine the diffusion coefficient of dopamine in the mouse nucleus accumbens core (NAcc) using a previously validated model.[22,23] We pharmacologically establish the dopaminergic nature of the chemical measurement *in vivo* by coupling FSCAV and FSCV. The power of this dual measurement at a single sensor is highlighted with pharmacological challenges that unveil the coaction of tonic and phasic dopamine *in vivo*.

Heien and co-workers first characterized FSCAV *in vitro*;[23] however, *in vivo* measurements are markedly more difficult because of the complex chemical environment of the brain. FSCAV is performed in three steps and takes a total of 20 seconds (Fig. 1 A). **1.** Minimizing adsorption by applying triangle waveform (−0.4 V to 1.3 V at 1200 V/s) every 10 ms for 2 seconds. **2.** Applying a constant potential (−0.4 V) to allow dopamine to adsorb on the electrode surface until it reaches equilibrium (10 seconds). **3.** Reapplying the triangle waveform and measuring the adsorbed dopamine (Γ_{DA}, 8 seconds). A color plot spanning one second directly following the time to reach equilibrium contains the raw data (Fig. 1B). The first scan following the controlled adsorption period includes signal from adsorbed dopamine and contains a large interference from the background change induced by the interruption of waveform application, complicating quantification of low levels of dopamine. In the previous *in vitro* study, following zero-phase filtering,[24] this background was removed using convolution theory[22] which provided more accurate results when compared to a simple subtraction.[23] Here, because of the differences in the shape of the *in vivo* background, matching the chemical composition of the brain environment *in vitro* is challenging. This limits the use of an *in vitro* principal component model to quantify *in vivo* signals.[25,26] Thus, it is necessary to define a method for analysis. In contrast to the first scan, by the second scan a peak is clearly visible, because the capacitive current from changing waveforms has decreased significantly, allowing the peak to be integrated to accurately quantify dopamine. There is a residual contribution from changes in the background visible in the one second section; however, this does not affect the precision of dopamine quantification by measuring the charge transferred during the oxidation wave. The limits for integration (vertical black dashed lines, Fig. 1C) are determined by examination of cyclic voltammograms obtained by electrical stimulation of the medial forebrain bundle (MFB), eliciting dopamine release. To validate that the sensor is capable of measuring *in vivo* concentrations of dopamine, Fig. 1D contains a calibration plot obtained post implantation. The sensitivity was 0.0078 ± 0.0002 pC/nM (n = 7 electrodes), and using Faraday's law to convert the signal to surface concentration, the sensitivity corresponds to b = 0.0037 ± 0.0002 cm (pmol/cm^{2}nM). The limit of detection is 3.4 ± 0.8 nM (n = 10 electrodes), which is sufficient for dopamine measurements *in vivo*. The tonic dopamine concentration in the nucleus accumbens of the mouse under urethane was determined to be 90 ± 9 nM (n = 20 animals) using FSCAV.

In the extracellular space, there are molecules present that have similar electroactive properties to dopamine. Specifically, DOPAC and ascorbic acid (AA) have historically confounded *in vivo* measurements.[27] FSCAV addresses selectivity in the following manner: First, dopamine cyclic voltammograms were distinguishable from those of DOPAC and

AA.[28] Second, our electrodes were coated with Nafion,[29] increasing selectivity for cations; Nafion limits the access of AA and DOPAC, both anionic species, to the electrode surface. Finally, due to the inherent chemical and electrochemical properties of the molecules, when the peak integrals from *in vitro* measurements were normalized to concentration, the ratio of the dopamine signal to DOPAC was 300 ± 20. The sensitivity to ascorbic acid was nearly zero, as the slope of the calibration curve was determined to be $2 \pm 2 \times 10^{-6}$ pC/nM. This shows that DOPAC and AA adsorb less strongly to CFMs than dopamine (Table S1). These effects, taken together, confer FSCAV with high selectivity for dopamine over DOPAC and AA.

During chemical communication, dopamine (a volume neurotransmitter) is released into the extracellular space where it diffuses to and interacts with distal receptors.[30–34] The distance of action is dependent upon the rate of mass-transfer and clearance mechanisms (*e.g.* metabolism, re-uptake). The ten-second controlled adsorption period is sufficient for dopamine adsorption at the electrode surface to reach equilibrium with the *in vivo* concentration (Fig. 2). In addition to enabling direct measurements of absolute concentrations, FSCAV measurements can be modeled using a previously developed finite-difference simulation to quantify mass-transport-limited adsorption dynamics using FSCAV.[23]

Experimentally, by varying the controlled adsorption period in Step 2 (*vide supra*, Fig. 1) from 0.1 to 20 seconds, the rate of mass transfer to the electrode can be quantified. For maximal sensitivity and precision, measurements made with FSCAV should be made at equilibrium. As seen in Fig. 2, the measured signal has reached equilibrium by ten seconds, as there is not a statistical difference between 10 seconds and 20 seconds ($p < 0.05$, Student t-test). By then fitting this data with our COMSOL model, a diffusion coefficient of $1.05 \pm 0.09 \times 10^{-6}$ cm^2/s (n = 4 animals, SEM) for dopamine ($R^2 = 0.98$) was measured and is consistent with previous results.[35–37] This provides an important metric for assessing tissue damage through its effect on the response time of a carbon-fiber microelectrode.

Pharmacological validation of *in vivo* FSCAV was performed by alternating measurements with background-subtracted fast-scan cyclic voltammetry (stimulated release, phasic) every five minutes after drug administration (time zero, Fig.3). While it may be possible to make FSCAV measurements every 20 seconds (can be made consecutively), the 5 minutes used in this work was chosen to allow time for the electrode to stabilize with the slower waveform application frequency (10 Hz) and scan rate (400 V/s) used for FSCV. This may be further optimized in future experiments, enabling rapid switching between the two methods. Dopamine concentrations are reported as a percent change from the mean pre-drug values; statistical significance is indicated by the horizontal bars above the data (Two-way analysis of variance, 2-way ANOVA, $p < 0.05$). We compared changes in dopamine between drug- and saline-treated mice, and found a significant interaction (drug and time) for normalized $[DA]_{tonic}$ ($F_{3,160} = 11.61$, $p < 0.001$) and $[DA]_{stimulated}$ ($F_{3,160} = 18.84$, $p < 0.001$). A Bonferoni correction post-hoc analysis was performed for each drug vs. saline to investigate the pharmacokinetics of each of the drugs in this study.

The effects of inhibiting dopamine synthesis with a tyrosine hydroxylase inhibitor, alpha-methyl-*p*-tyrosine (AMPT, *i.p.* 250 mg kg^{-1}), was investigated (Fig. 3A). Both stimulated and tonic dopamine decreased by 55 ± 15 % (35 min, Bonferoni post-hoc, $p < 0.001$) and 20 ± 10 % (30 min, Bonferoni post-hoc, $p < 0.01$), respectively. The changes in tonic dopamine measured by FSCAV and changes in dopamine efflux as measured by FSCV is equivalent to results shown previously.[38–40] The partial reduction of dopamine induced by AMPT is not unexpected. Acute AMPT administration does not cause complete depletion of dopamine; which may be the result of differences in contributions from vesicular and cystolic pools of dopamine to the tonic concentration.[41,42] To further investigate these findings, future work should include studying the effects of tetrodotoxin or kynurenate.[15,43,44] Next, we targeted the dopamine transporter (DAT) with GBR-12909 (*i.p.* 10 mg kg^{-1}) which led to an increase in $[DA]_{tonic}$ of 130 ± 70 % (80 min, Bonferoni post-hoc, $p < 0.01$) and $[DA]_{stimulated}$ of 260 ± 150 % (75 min, Bonferoni post-hoc, $p < 0.001$) (Fig. 3B). Finally, dopamine metabolism was inhibited with pargyline hydrochloride (*i.p.* 75 mg kg^{-1}), an inhibitor of monoamine oxidase (MAO), which converts dopamine to DOPAC (Fig. 3C). Here we found an increase in $[DA]_{tonic}$ of 120 ± 70 % (90 min, Bonferoni post-hoc, $p < 0.001$) and $[DA]_{stimulated}$ of 80 ± 20 % (85 min Bonferoni post-hoc, $p < 0.001$). This experiment validates that there is minimal contribution to our measured signal from DOPAC to the FSCAV signal. The increases in the FSCAV signal after pargyline are consistent with the drug's effects on dopamine (inhibition of metabolism, therefore an increase in dopamine levels) and inconsistent with its effect on DOPAC (inhibition of DOPAC production, therefore a decrease in DOPAC concentrations).

These pharmacological challenges validate that the chemical nature of the measured signal is dopaminergic and demonstrate that coupling FSCAV and FSCV enables the relationships between tonic and phasic signaling to be studied. By comparing changes in the stimulated dopamine response with changes in tonic dopamine levels, significant correlations are reported (Fig.S1). As expected, stimulated dopamine release and tonic dopamine levels do not correlate when saline is administered ($R^2 = 0.17$, $p = 0.26$). Interestingly, pargyline ($R^2 = 0.95$, $p < 0.0001$), GBR-12909 ($R^2 = 0.88$, $p = 0.0002$) and AMPT ($R^2 = 0.56$, $p = 0.032$) yielded significant correlations. This multi-dimensional temporal analysis illustrates the intricate interplay of tonic and phasic signaling and has transformative implications for enriching our understanding of neuromodulator mechanisms.

Conclusions

Dopamine dynamics include fast responses to salient stimuli and slow changes in extracellular tonic concentrations. Here we validated and used FSCAV to provide measurements of local tonic dopamine with high temporal resolution. We found, using FSCAV that the tonic dopamine concentration in the NAc of anesthetized mice is 90 ± 9 nM. FSCAV and FSCV were then coupled at the same sensor to study how pharmacological inhibition of dopamine synthesis, reuptake, or metabolism affects the tonic and phasic dopamine neurotransmission. FSCAV is easily implemented with existing FSCV instrumentation, enabling tonic dopamine measurements within seconds. We have shown that when FSCAV and FSCV are coupled, a full spectrum of dopamine temporal dynamics can be studied *in vivo* at a single sensor. This sensing platform has the potential to elucidate

the signaling dynamics of any adsorbing electroactive neurotransmitters (*e.g.* dopamine, serotonin, and norepinephrine) in various preparations. Specifically, the method shows great promise for studying biogenic amine signaling *in vitro* as the buffer constituents are precisely controlled thus enabling complete removal of the background interference by convolution theory. Additionally this method has potential in evaluating preclinical models of neurological disorders such as Parkinson's disease, attention deficit hyperactivity disorder, or schizophrenia where tonic levels are implicated.

Supplementary Material

Refer to Web version on PubMed Central for supplementary material.

Acknowledgments

The authors thank Janusz Lipski for helpful comments. This work was supported by the University of Arizona and Wayne State University. Kate L. Parent was supported by a Department of Chemistry and Biochemistry Summer Research Assistantship Award.

Notes and References

1. Grace AA. Addiction. 2000; 95(Suppl 2):S119–S128. [PubMed: 11002907]
2. Dreyer JK, Herrik KF, Berg RW, Hounsgaard JD. J. Neurosci. 2010; 30:14273–14283. [PubMed: 20962248]
3. Schultz W. Annu. Rev. Neurosci. 2007; 30:259–288. [PubMed: 17600522]
4. Schultz W. J. Neurophysiol. 1998; 80:1–27. [PubMed: 9658025]
5. Baik JH, Picetti R, Saiardi A, Thiriet G, Dierich A, Depaulis A, Le Meur M, Borrelli E. Nature. 1995; 377:424–428. [PubMed: 7566118]
6. Salamone JD, Correa M, Mingote SM, Weber SM. Curr. Opin. Pharmacol. 2005; 5:34–41. [PubMed: 15661623]
7. Parsons LH, Justice JB. J. Neurochem. 1992; 58:212–218. [PubMed: 1727431]
8. Chefer VI, Zapata A, Shippenberg TS, Bungay PM. J. Neurosci. Methods. 2006; 155:187–193. [PubMed: 16466808]
9. Stenken JA. Anal. Chim. Acta. 1999; 379:337–358.
10. Marsden CA, Joseph MH, Kruk ZL, Maidment NT, O'Neill RD, Schenk JO, Stamford JA. Neuroscience. 1988; 25:389–400. [PubMed: 3041309]
11. Huffman ML, Venton BJ. Analyst. 2009; 134:18–24. [PubMed: 19082168]
12. Millar J. Methods Mol. Biol. 1997; 72:251–266. [PubMed: 9249752]
13. Kuhr WG, Wightman RM. Brain Res. 1986; 381:168–171. [PubMed: 3489505]
14. Owesson-White CA, Roitman MF, Sombers LA, Belle AM, Keithley RB, Peele JL, Carelli RM, Wightman RM. J. Neurochem. 2012; 121:252–262. [PubMed: 22296263]
15. Borland LM, Michael AC. J. Neurochem. 2004; 91:220–229. [PubMed: 15379902]
16. Dreyer JK, Hounsgaard J. J. Neurophysiol. 2013; 109:171–182. [PubMed: 23054599]
17. Justice JB. J. Neurosci. Methods. 1993; 48:263–276. [PubMed: 8105154]
18. Peters JL, Miner LH, Michael AC, Sesack SR. J. Neurosci. Methods. 2004; 137:9–23. [PubMed: 15196823]
19. Nesbitt KM, Jaquins-Gerstl A, Skoda EM, Wipf P, Michael AC. Anal. Chem. 2013; 85:8173–8179. [PubMed: 23927692]
20. Lama RD, Charlson K, Anantharam A, Hashemi P. Anal. Chem. 2012; 84:8096–8101. [PubMed: 22881278]
21. Howell JO, Kuhr WG, Ensman RE, Mark Wightman R. J. Electroanal. Chem. Interfacial Electrochem. 1986; 209:77–90.

22. Atcherley CW, Laude ND, Monroe EB, Wood KM, Hashemi P, Heien ML. ACS Chem. Neurosci. 2014
23. Atcherley CW, Laude ND, Parent KL, Heien ML. Langmuir. 2013; 29:14885–14892. [PubMed: 24245864]
24. Atcherley CW, Vreeland RF, Monroe EB, Sanchez-Gomez E, Heien ML. Anal. Chem. 2013; 85:7654–7658. [PubMed: 23919317]
25. Heien MLV, Khan AS, Ariansen JL, Cheer JF, Phillips PEM, Wassum KM, Wightman RM. Proc. Natl. Acad. Sci. U. S. A. 2005; 102:10023–10028. [PubMed: 16006505]
26. Heien MLAV, Johnson MA, Wightman RM. Anal. Chem. 2004; 76:5697–5704. [PubMed: 15456288]
27. Cahill PS, Walker QD, Finnegan JM, Mickelson GE, Travis ER, Wightman RM. Anal. Chem. 1996; 68:3180–3186. [PubMed: 8797378]
28. Heien MLAV, Johnson MA, Wightman RM. Anal. Chem. 2004; 76:5697–5704. [PubMed: 15456288]
29. Gerhardt GA, Oke AF, Nagy G, Moghaddam B, Adams RN. Brain Res. 1984; 290:390–395. [PubMed: 6692152]
30. Syková E, Nicholson C. Physiol. Rev. 2008; 88:1277–1340. [PubMed: 18923183]
31. Cragg SJ, Rice ME. Trends Neurosci. 2004; 27:270–277. [PubMed: 15111009]
32. Jennings KA. ACS Chem. Neurosci. 2013; 4:704–714. [PubMed: 23627553]
33. Nicholson, C.; Rice, ME. Volume transmission in the brain. Vol. 1. Diffusion of ions and transmitters in the brain cell microenvironment: Raven Press; 1991. p. 279-294.
34. Rice ME. Prog. Brain Res. 2000; 125:277–290. [PubMed: 11098664]
35. Venton BJ, Zhang H, Garris PA, Phillips PEM, Sulzer D, Wightman RM. J. Neurochem. 2003; 87:1284–1295. [PubMed: 14622108]
36. Nicholson C. Biophys. J. 1995; 68:1699–1715. [PubMed: 7612814]
37. Rice ME, Gerhardt GA, Hierl PM, Nagy G, Adams RN. Neuroscience. 1985; 15:891–902. [PubMed: 2866468]
38. Park J, Kile BM, Wightman RM. Eur. J. Neurosci. 2009; 30:2121–2133. [PubMed: 20128849]
39. Watanabe S, Fusa K, Takada K, Aono Y, Saigusa T, Koshikawa N, Cools AR. J. Oral Sci. 2005; 47:185–190. [PubMed: 16415562]
40. Fulford AJ, Marsden CA. Neuroscience. 2007; 149:392–400. [PubMed: 17869434]
41. Ewing AG, Bigelow JC, Wightman RM. Science. 1983; 221:169–171. [PubMed: 6857277]
42. Yavich L. Br. J. Pharmacol. 1996; 119:869–876. [PubMed: 8922734]
43. Smith AD, Justice JB. J. Neurosci. Methods. 1994; 54:75–82. [PubMed: 7815821]
44. Westerink BH, De Vries JB. J. Neurochem. 1988; 51:683–687. [PubMed: 3411321]

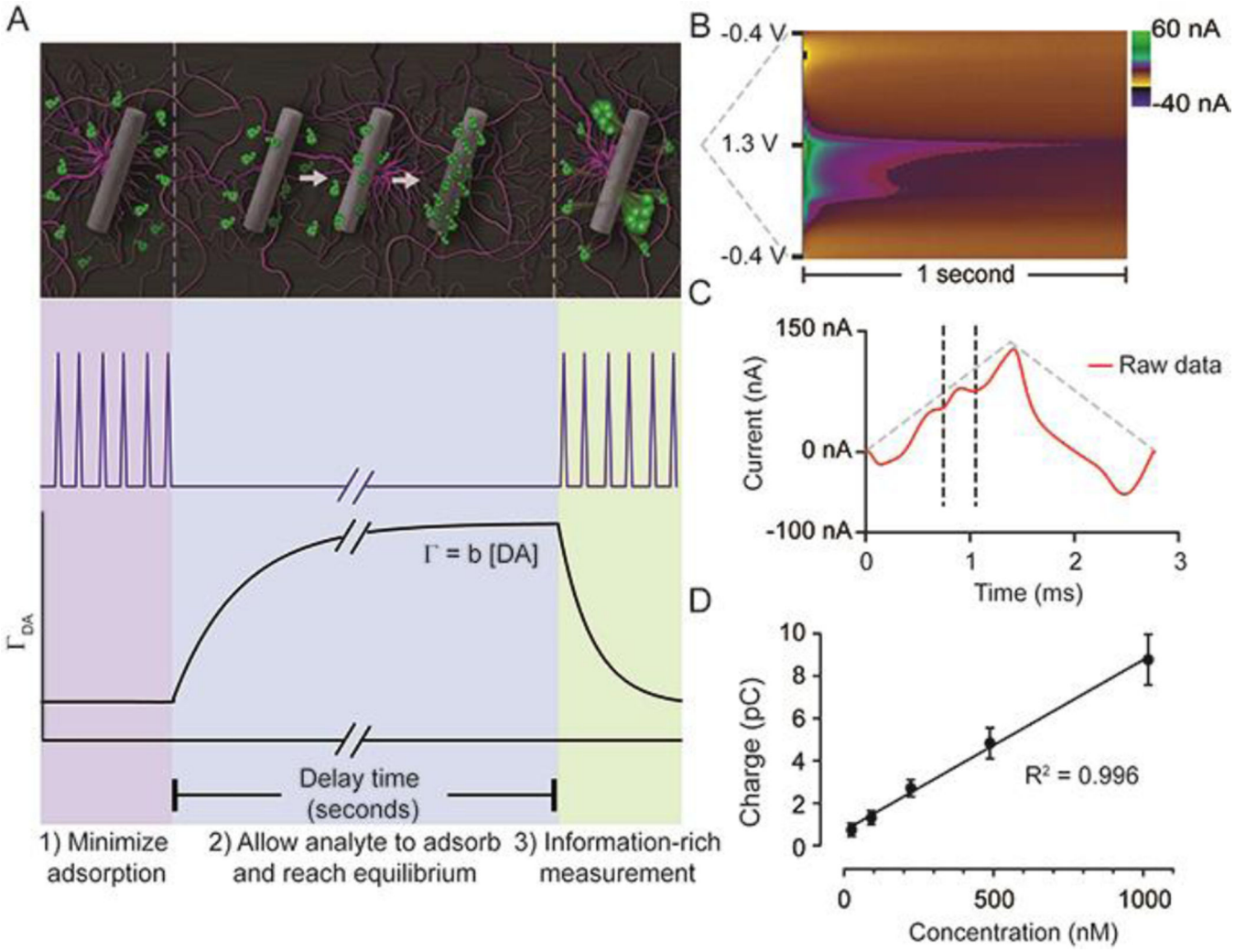

Fig. 1.

FSCAV was carried out in 3 steps (A): 1) The waveform was applied every 10 ms which minimizes dopamine adsorption to the electrode. 2) The potential was held at −0.4 V for 10 seconds to allow dopamine to adsorb to the electrode and reach equilibrium. 3) The waveform was reapplied, and the adsorbed dopamine was measured. Surface-accumulated dopamine (Γ_{DA}) is proportional to the tonic concentration [DA] by the strength of adsorption (b). (B) Resultant color plot from step 3, with voltage on the ordinate, time on the abscissa, and current displayed using false colors. (D) Representative current trace (red) taken 10 ms after the beginning of step 3. The vertical dashed lines show the bounds for integration to quantify adsorbed dopamine. The grey-dashed triangles illustrate the voltage waveform applied. (D) A calibration plot obtained by FSCAV post implantation ($R^2 = 0.996$, slope = 0.0078 ± 0.0002 pC/nM (n = 7 electrodes), which when accounting for electrode area and equivalents transferred, corresponds to b = 0.0037 ± 0.0002 cm.

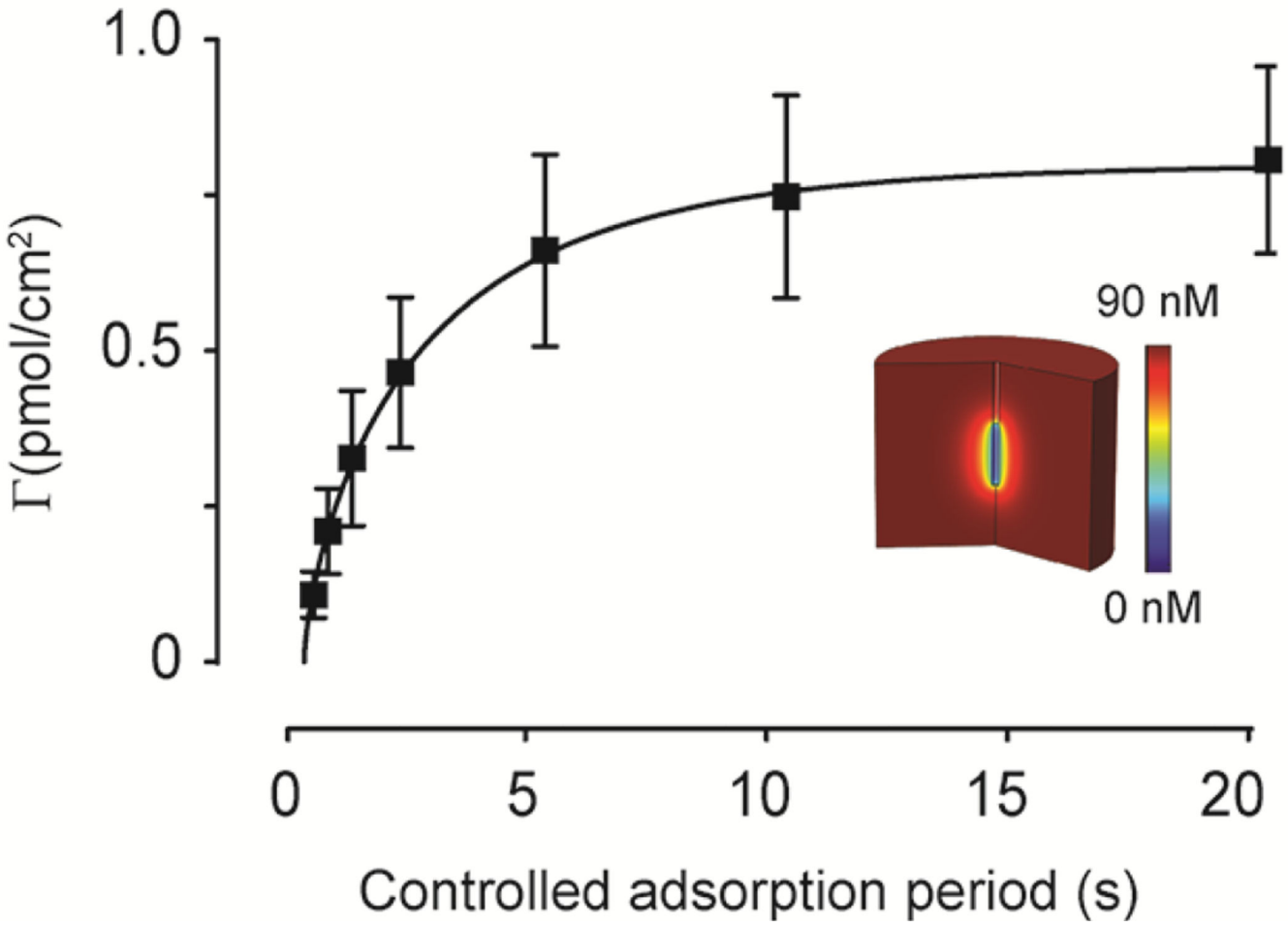

Fig. 2.

FSCAV is used to determine the diffusion coefficient of endogenous dopamine *in vivo*. The controlled adsorption period is varied and the amount of adsorbed dopamine vs. time is plotted (n = 4 mice). Using a finite-difference simulation (inset), the data is fit (red line), and a diffusion coefficient is determined ($1.05 \pm 0.09 \times 10^{-6}$ cm^2/s).

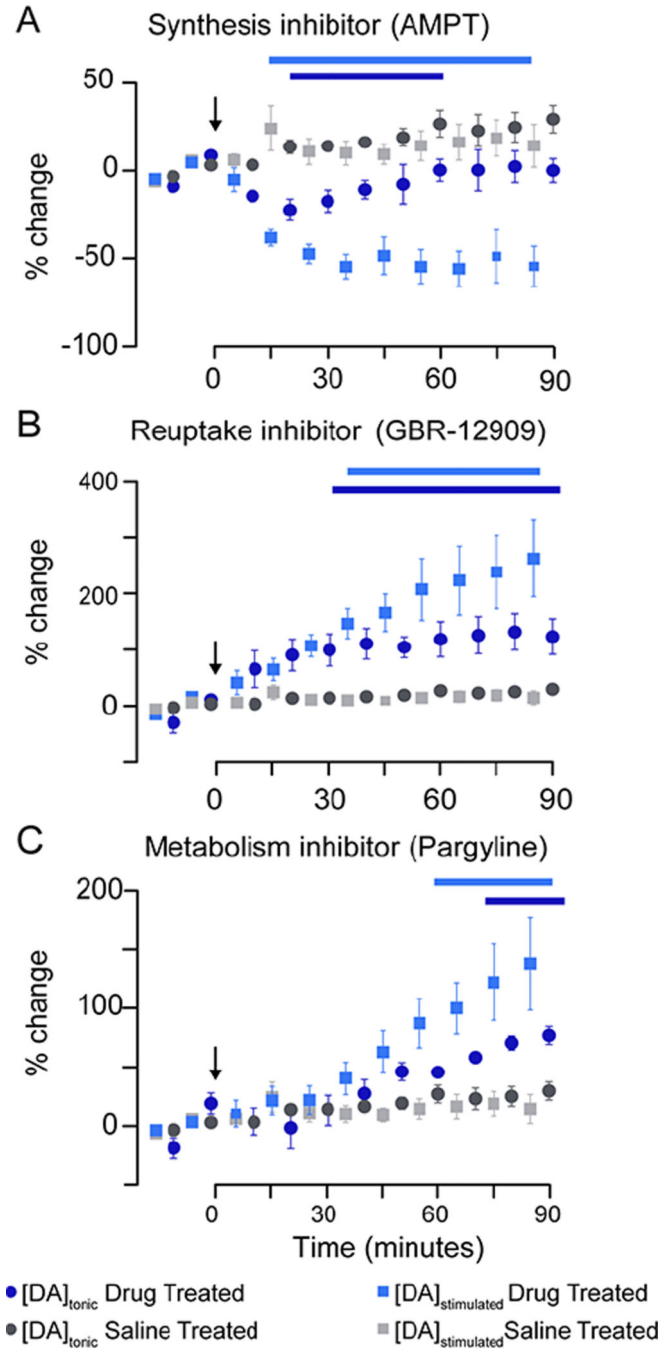

Fig. 3.

Pharmacological effects on tonic dopamine concentrations and electrically evoked dopamine release. Changes in stimulated release and tonic concentration are plotted as the percent change from baseline vs. time. Measurements began 30 minutes prior to drug administration starting with tonic measurements alternated with stimulated release measurements (every 5 minutes). The changes in electrically evoked dopamine release (blue squares) and the tonic concentration (blue circles) of dopamine in response to (A) AMPT (250 mg/kg, *i.p.*), (B) GBR-12909 (10 mg/kg, *i.p.*), and (C) pargyline (75 mg/kg, *i.p.*) are shown (n = 5 mice, each

group). Each plot contains the saline controls (gray). Bars above plot indicate significant differences when compared to saline controls ($p < 0.05$)